Renewable and Sustainable Energy Reviews 34 (2014) 578–587

Contents lists available at ScienceDirect

Renewable and Sustainable Energy Reviews

journal homepage: www.elsevier.com/locate/rser

Mathematical models for efficiency of inverters used in grid connected photovoltaic systems

G.A. Rampinelli [a], A. Krenzinger [b], F. Chenlo Romero [c]

[a] Federal University of Santa Catarina (UFSC), Rodovia Governador Jorge Lacerda, 3201 Araranguá, SC, Brazil
[b] Federal University of Rio Grande do Sul (UFRGS), Avenida Bento Gonçalves, 9500 Porto Alegre, RS, Brazil
[c] Research Centre for Energy, Environment and Technology (CIEMAT), Avenida Complutense, 22, Madrid, Spain

ARTICLE INFO

Article history:
Received 16 November 2013
Received in revised form
28 February 2014
Accepted 9 March 2014
Available online 4 April 2014

Keywords:
Solar energy
Grid connected photovoltaic system
Inverters
Software

ABSTRACT

In order to perform a reliable simulation of a photovoltaic system is crucial to know the electrical and thermal characteristics of each component that will be modeled by mathematical models that describe the system operation. This paper presents the development of mathematical models that characterize the inverter used in grid-connected photovoltaic systems. The mathematical models were fitted from experimental tests and they are suitable to be used in computer simulation software. The tests were performed on a set of inverters commercially available at Solar Energy Laboratory at Federal University of Rio Grande do Sul (UFRGS, Brazil) and at Photovoltaic Solar Energy Laboratory at Research Centre for Energy, Environment and Technology (CIEMAT, Spain). From the measured data it was calculated fitting coefficients to the efficiency curve of several inverters. In order to use these mathematical models for simulating other inverters, their own coefficients have to be experimentally determined and entered into the data base of the software in order to provide a full detailed computer simulation.

Contents

1. Introduction

The evaluation of a grid connected photovoltaic system can be accomplished through a long time or short time monitoring system [1]. It is fundamental to investigate and emphasize the importance of the grid connected PV system regarding the intermittent nature of renewable generation, and the characterization of PV generation with regard to grid code compliance [2]. Software is an important tool for simulation, design, characterization and analysis of photovoltaic systems. The monitoring equipment depends on experimental measurements and time to perform the system analysis in a short time, while computer software has the capability to perform a number of simulations of

E-mail addresses: giuliano.rampinelli@ufsc.br (G.A. Rampinelli), arno.krenzinger@ufrgs.br (A. Krenzinger), faustino.chenlo@ciemat.es (F. Chenlo Romero).

http://dx.doi.org/10.1016/j.rser.2014.03.047
1364-0321/© 2014 Published by Elsevier Ltd.

different configurations. However, to perform a simulation that return reliable data is necessary to use software that incorporates mathematical models capable of describing accurately the behavior of the components of a photovoltaic system. These models must be experimentally validated and obtained from specific tests.

Grid connected photovoltaic system does not use batteries to energy storage and the electricity output varies throughout the day. This means that there is little influence of prior history to determine what happens in the time interval being analyzed. At intervals of about 1 min, the memory of the past behavior is restricted to the thermal effects considered in modules and inverters. Except for these, it can be said that the electrical energy injected on the grid is dependent on only a set of variables and parameters defined instantaneously. In fact it would be enough to establish the temperature values for modules and inverters and the solar irradiance as parameters for a set of equations for the entire simulation.

2. The inverter

The inverter converts DC power from the PV system on AC power that will be injected into the grid. The development of electronic technology has allowed considerable increase in the conversion efficiency, together with increased reliability and reduced costs.

\Historically, low power photovoltaic systems use single-phase inverters. In grid connected applications, the single-phase inverters produce an imbalance between the phases by injecting current into only one phase of the grid. Due to stability reasons, it is possible to connect a maximum power of 4.6 kW, with 10% of tolerance, at one stage to avoid a greater asymmetry between the phases of the grid [3]. For power greater than 5 kW three single-phase inverters are needed to ensure a balanced distribution between the three phases [3]. The inverters used in grid connected photovoltaic systems use different circuits for energy conversion and there are a number of options of transformer configuration. There are commercial inverters with high or low frequency transformers and even transformerless inverters. Each topology has its own characteristics, resulting in advantages and disadvantages [4–9]. The inverters used in grid-connected applications embed maximum power point tracker, anti-islanding operation, high conversion efficiency, automatic synchronization with the grid and they have low level of harmonics distortion and power factor close to unity [10–12]. The performance of the inverters connected to the grid depends largely on the control strategy applied [13,14].

2.1. DC to AC conversion efficiency

The DC to AC conversion efficiency of the inverter (Eq. (1)) is set as the ratio between the output power of the inverter and the input power of the inverter [15].

$$\eta_{inv}=\frac{E_{AC}}{E_{DC}}=\frac{\int P_{AC}\,dt}{\int P_{DC}\,dt} \tag{1}$$

where E_{AC} is the output electrical energy; E_{DC} is the input electrical energy, P_{AC} is the output power and P_{DC} is the input power.

The European efficiency and Californian Efficiency are defined based on weighting of inverter efficiency for different powers Eqs. (2) and (3).

$$\eta_{EU}=(0.03\eta_{5\%})+(0,06\eta_{10\%})+(0.13\eta_{20\%}) +(0.1\eta_{30\%})+(0.48\eta_{50\%})+(0.2\eta_{100\%}) \tag{2}$$

$$\eta_{CAL}=(0.04\eta_{10\%})+(0.05\eta_{20\%})+(0.12\eta_{30\%}) +(0.21\eta_{50\%})+(0.53\eta_{75\%})+(0.05\eta_{100\%}) \tag{3}$$

where $\eta_{5\%}$, $\eta_{10\%}$, $\eta_{20\%}$, $\eta_{30\%}$, $\eta_{50\%}$, $\eta_{75\%}$ and $\eta_{100\%}$ are the values of conversion efficiency, respectively 5%, 10%, 20%. 30%, 50%, 75% and 100% rated power of the inverter.

The DC to AC conversion efficiency is strongly dependent on the relative power. The DC voltage also affects the conversion efficiency, although this dependence is often overlooked in the simplest mathematical models that represent the electrical behavior of the inverter. The efficiency also has temperature dependence, although it is advisable not to disregard this dependence increase the complexity of the mathematical model. Tests conducted at Sandia National Laboratories show that the DC to AC efficiency has negligible dependence with the temperature [16]. Mathematical models of inverters, usually determine the conversion efficiency using different parameters associated with thermal and electrical losses resulting from the conversion process.

A model found in the literature suggests that the efficiency can be obtained from the interpolation of experimental data [17]. The efficiency for a given power is determined Eq. (4) by linear interpolation within a given power range, where the efficiencies of the inverter correspondent to the lower limit and to the upper limit of power are known.

$$\eta_{inv}=\eta_{inf}+\frac{(P_{AC}-P_{inf})(\eta_{sup}-\eta_{inf})}{(P_{sup}-P_{inf})} \tag{4}$$

where P_{inf} is the lower limit of power; P_{sup} is the upper limit of power; η_{inf} is the inverter efficiency in the lower limit of power and η_{sup} is the inverter efficiency in the upper limit of power.

Another proposed model for the efficiency Eq. (5) is based on the equivalent circuit consisting of an ideal inverter, a series resistance that represents the ohmic losses and a parallel resistor which represent the self-consumption [18].

$$\eta_{inv}=\frac{2R_SP_{AC}}{V_{DC}^2}\frac{1}{1-\sqrt{1-4\left(R_S/V_{DC}^2\right)\left(P_{AC}+\left(V_{AC}^2/R_P\right)\right)}} \tag{5}$$

where V_{DC} is the input voltage of the inverter; V_{AC} is the output voltage of the inverter; R_S is the series resistance; R_P is the parallel resistance.

The model can be extended also to reactive loads Eq. (6) considering the apparent power and including a factor that has a value close to unity except for very low power factors and also represents additional losses due to high internal reactive currents.

$$\eta_{inv}=\frac{2R_SS}{V_{DC}^2}\frac{a}{1-\sqrt{1-4\left(R_S/V_{DC}^2\right)\left(P_{AC}+\left(V_{AC}^2/R_P\right)\right)}} \tag{6}$$

Another model found in the literature is a simple mathematical model where the lost converting energy is represented by a polynomial [19]. The model coefficients are associated with different sources of electrical losses of the inverters Eq. (7).

$$\eta_{inv}=\frac{(P_{AC}/P_{NOM})}{(P_{AC}/P_{NOM})+(K_0+K_1(P_{AC}/P_{NOM})+K_2(P_{AC}/P_{NOM})^2)} \tag{7}$$

where K_0, K_1 and K_2 are mathematical coefficients and P_{NOM} is the nominal power of the inverter.

A mathematical model to describe the performance of inverters used in grid connected photovoltaic systems was empirically developed. From the relationship between the P_{DC} and P_{AC} the model coefficients are determined Eqs. (8) and (9) [16].

$$P_{AC}=\left(\frac{P_{ACO}}{(A-B)}-C(A-B)\right)(P_{DC}-B)+C(P_{DC}-B)^2 \tag{8}$$

$$A=P_{DCO}(1+C_1(V_{DC}-V_{DCO})),\quad B=P_{SO}(1+C_2(V_{DC}-V_{DCO})),\quad C=C_0(1+C_3(V_{DC}-V_{DCO})) \tag{9}$$

where P_{AC} is the output power of the inverter; P_{ACO} is the output maximum power of the inverter; P_{DC} is the input power of the

inverter; V_{DC} is the input voltage of the inverter; V_{DCO} is the nominal voltage; P_{SO} is the power that the inverter comes into operation; C_0 is the angular coefficient of the relationship between AC power and DC power; C_1, C_2 *e* C_3 are coefficients experimentally determined.

2.2. Maximum power point tracker efficiency

To maximize the conversion of solar energy into electricity the inverters present algorithms for maximum power point tracker (MPPT). The maximum power point tracker efficiency is defined [20,21] as the ratio between the input power of the inverter and the power that the inverter would convert if operating ideally at the maximum power point (Eq. (10)).

$$\eta_{MPPT} = \frac{E_{DC}}{E_{MPP}} = \frac{\int P_{DC}\,dt}{\int P_{MPP}\,dt} \tag{10}$$

where η_{MPPT} is the maximum power point tracker efficiency; E_{DC} is the electrical energy with actual MPPT; E_{MPP} is the electrical energy with ideal MPPT.

The importance of this issue is evidenced by the large number of scientific papers published [22–30]. A comprehensive presentation of working principle of these techniques is presented in [31]. They are compared against each other in terms of some critical parameters like number of variables used, complexity, accuracy, speed, hardware implementation, cost and tracking efficiency [31]. The difficulty in determining the MPPT efficiency from experimental tests is subject to the accuracy of the measurement of the maximum power point of the PV system. There are several methodologies that propose the determination of that power. Analytical methods are based on mathematical models while empirical models using data on specific tests [32,33]. The maximum power point can be determined by Eq. (11).

$$P_{MPP} = P_{FV}^{0} \cdot \frac{G_{t,\beta}}{G_{ref}} \cdot [1 - \gamma_{MPP}(T_{MC} - T_{MC,ref})] \tag{11}$$

where P_{MPP} is the maximum power point; P_{FV} is the PV array power in the standard conditions; $G_{t,\beta}$ is the irradiance in the measurement condition; T_{MC} is the module temperature in the measurement condition; G_{ref} is the standard irradiance (1000 W/m^2); $T_{MC,ref}$ is the standard module temperature (25 °C) and γ_{MPP} is the temperature coefficient of the maximum power point.

3. Experimental methodology

Experimental tests were divided in two stages. The first stage of work was developed at the Solar Energy Laboratory (LABSOL) at Federal University of Rio Grande do Sul (UFRGS). The PV system has a power of 4.8 kWp and is composed of modules manufactured by Isofoton (I-100/24) that have rated power of 100 Wp. For those specific tests were used 10 different models of inverters, five from SMA technology, three Fronius technology and two Mastervolt technology and it was assembled a test bench consisting of a power analyzer and a computer to acquire data. The electrical characteristics analyzed were conversion efficiency and MPPT efficiency. The physical quantities measured were DC voltage and current and AC voltage and current. The Table 1 presents the main technical characteristics of the inverters used in the tests developed at LABSOL/UFRGS [34–40].

The second stage of the work was developed at Photovoltaic Solar Energy Laboratory at Research Centre for Energy, Environment and Technology (CIEMAT). The photovoltaic system at CIEMAT is rated at 3 kW. To monitor and measure the electrical characteristics of the system it was necessary to assemble and install a measurement system. This system consists of a power analyzer and a laptop which communicates with the devices through specific software. To perform the electrical testing of inverters used in grid connected photovoltaic systems, seven models of single-phase inverters from different manufacturers were used, as well as three inverters SMA technology and inverters from the following manufacturers: Ingeteam, Fronius, Xantrex and Sunways. Table 2 presents some inverter electrical characteristics used in the tests of conversion efficiency at different DC input voltage [34,39–43].

4. Inverters mathematical model

The main inverters electrical characteristics for grid connection are DC to AC conversion efficiency, MPPT efficiency, power factor and harmonic distortion [44]. The mathematical models developed were obtained by testing different technologies. The coefficients of the mathematical models are obtained from the fitting between the experimental data and the theoretical curve provided by the mathematical model.

4.1. Mathematical model of DC to AC conversion efficiency

This study adopts the first mathematical model Eq. (7) for description of the inverter conversion efficiency [13]. The efficiency is measured across the range of admissible power of the inverter, resulting in an efficiency curve as a function of relative power. The power coefficients are obtained from the fit of the measured points and the theoretical curve provided by the mathematical model. Fig. 1 shows the measured conversion efficiency curve of the inverter SMA Sunny Boy 700U and the adjustment of the curve described by the theoretical mathematical

Table 1
DC and AC power data of inverters that were tested at LABSOL/UFRGS.

Technology	Model	DC power (W)		AC power (W)		Transformer
		Maximum	Nominal	Maximum	Nominal	
SMA	*SB* 700*U*	1000	780	700	700	Low frequency
SMA	*SB* 1100*E*	1210	1100	1100	1000	Low frequency
SMA	*SB* 2100	2450	2000	2100	1900	Low frequency
SMA	*SB* 2500	3000	2480	2500	2300	Low frequency
SMA	*SB* 3800*U*	4800	4040	3800	3800	Low frequency
Fronius	*IG* 15	2000	1400	1500	1300	High frequency
Fronius	*IG* 20	2700	1940	2000	1800	High frequency
Fronius	*IG* 30	3600	2690	2650	2500	High frequency
Mastervolt	*QS* 2000	1800	1700	1725	1600	High frequency
Mastervolt	*QS* 3200	2950	2750	2750	2600	High frequency

Table 2
DC and AC power data of inverters that were tested at CIEMAT.

Technology	Model	DC Power (kW)		AC Power (kW)		Transformer
		Maximum	Nominal	Maximum	Nominal	
Ingeteam	*Ingecon Sun* 2,5	3.3	3.3	2.7	2.5	Low frequency
SMA	*SB* 1100U	1.21	1.2	1.1	1.0	Low frequency
Fronius	*IG* 30	3.6	2.69	2.65	2.5	High frequency
Sunways	*NT* 4000	3.4	3.4	3.3	3.3	Transformerless
Xantrex	*GT* 3.0	3.4	3.4	3.3	3.3	High frequency
SMA	*SB* 3300*TL*	3.44	3.44	3.3	3.0	Transformerless
SMA	*SB SWR* 2000	2.1	2.1	2.0	1.8	Low frequency

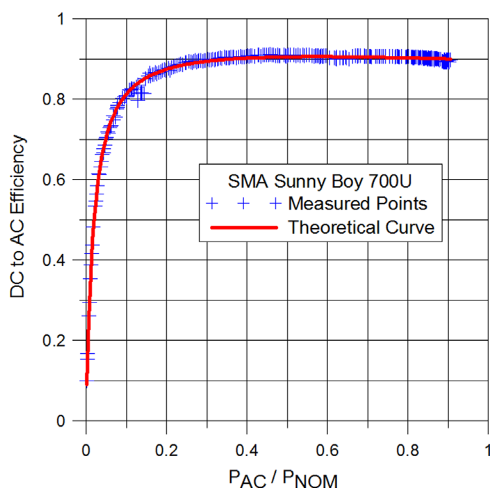


Fig. 1. DC to AC conversion efficiency curve of the inverter SMA Sunny Boy 700U.

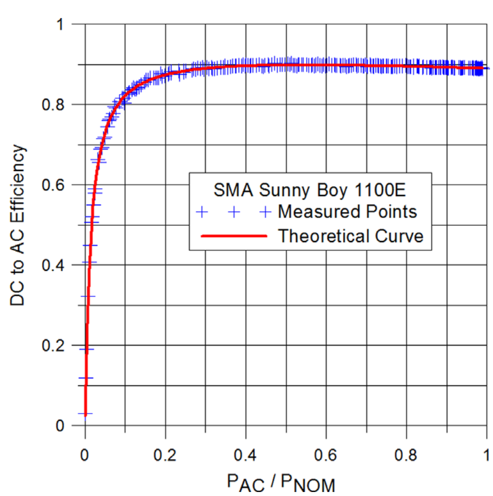


Fig. 2. DC to AC conversion efficiency curve of the inverter SMA Sunny Boy 1100E.

model. Fig. 2 shows the conversion efficiency curve of the inverter SMA Sunny Boy 1100E.

Table 3 shows the coefficients derived from the agreement between the measured points and the theoretical curve provided by the mathematical model and Table 4 shows the inverters efficiency tested for each power value set efficiency in the European and Californian efficiency.

The shape of the curves of conversion efficiency follows the expected behavior. The fit between the curve described by the mathematic model and the measured data has a coefficient of determination R^2 greater than 0.9 for all inverters tested. In general, from 30% of the rated power, the conversion efficiency is around 90% and maximum values of efficiency are obtained in relative power between 0.5 and 0.8, with the exception of the inverter SMA Sunny Boy 2500 which has its maximum efficiency at loading levels of about 30%. The efficiency decreases for lower power, because all devices have a minimum power self-consumption whose proportion obviously increases as the power decreases. The European and California efficiencies differ in the values of power factors considered and the corresponding

Table 3
Power coefficients of the conversion efficiency mathematical model.

Technology	Model	K_0	K_1	K_2	R^2
SMA	*SB* 700*U*	0.0185	0.0393	0.0562	0.99
SMA	*SB* 1100*E*	0.0154	0.0562	0.0519	0.99
SMA	*SB* 2100	0.0139	0.0395	0.0465	0.99
SMA	*SB* 2500	0.0042	0.0327	0.0635	0.91
SMA	*SB* 3800*U*	0.0187	0.0368	0.044	0.99
Fronius	*IG* 15	0.0209	0.0895	−0.0113	0.97
Fronius	*IG* 20	0.0349	0.057	0.0218	0.99
Fronius	*IG* 30	0.0205	0.0438	0.0477	0.95
Mastervolt	*QS* 2000	0.0164	0.0696	0.0199	0.99
Mastervolt	*QS* 3200	0.0201	0.0606	0.0366	0.98

Table 4
Tested inverters efficiency for each power value set in the European and Californian efficiency.

Model	5%	10%	20%	30%	50%	75%	100%
SB 700*U*	70.8	81.3	87.4	89.4	90.5	90.4	89.7
SB 1100*E*	73.1	82.2	87.4	89.0	89.8	89.6	89.0
SB 2100	75.7	84.5	89.4	90.9	91.6	91.4	90.9
SB 2500	89.2	92.5	93.7	93.8	93.2	92.0	90.8
SB 3800*U*	70.7	81.4	87.7	89.9	91.2	91.3	90.9
IG 15	66.3	77.0	83.9	86.5	88.8	90.1	90.9
IG 20	56.9	71.0	80.9	84.7	87.8	89.2	89.7
IG 30	68.6	79.7	86.5	88.7	90.1	90.3	89.9
QS 2000	71.5	80.9	86.5	88.4	89.8	90.3	90.4
QS 3200	68.2	79.0	85.5	87.8	89.3	89.6	89.5

Table 5
European and Californian efficiency of the tested inverters.

Technology	Model	η_{EU}	η_{CAL}
SMA	*SB* 700*U*	88.7	89.2
SMA	*SB* 1100*E*	88.3	88.3
SMA	*SB* 2100	90.2	90.4
SMA	*SB* 2500	92.7	92.0
SMA	*SB* 3800*U*	89.3	90.0
Fronius	*IG* 15	86.9	87.4
Fronius	*IG* 20	85.1	86.5
Fronius	*IG* 30	88.2	88.8
Mastervolt	*QS* 2000	88.3	88.5
Mastervolt	*QS* 3200	87.4	87.9

multipliers and are usually taken as representative for the average irradiance levels medium and high, respectively. Table 5 shows the European and Californian efficiency of the tested inverters at LABSOL/UFRGS.

4.2. Study of DC to AC conversion efficiency as function of input voltage

The conversion efficiency is mainly dependent on the loading level of the inverter. However the DC input voltage also affects the conversion efficiency of inverter. To analyze the influence of DC input voltage on the behavior of the conversion efficiency, tests were carried out for single-phase inverter power rating up to 5 kW at different DC voltages. The conversion efficiency depends on the DC input voltage and thus the mathematical model representing the curve of the conversion efficiency must consider corresponding dependence of coefficients on the DC input voltage. This paper proposes a modification to the model of the Eq. (7), inserting voltage-dependent coefficients Eq. (12).

$$\eta_{inv} = \frac{(P_{AC}/P_{NOM})}{(P_{AC}/P_{NOM})+(K_0(V_{DC})+K_1(V_{DC})(P_{CA}/P_{NOM})+K_2(V_{DC})(P_{CA}/P_{NOM})^2)} \quad (12)$$

where $K_0(V_{DC})$, $K_1(V_{DC})$ and $K_2(V_{DC})$ are power coefficients of proposed mathematical model.

The curve of conversion efficiency of the inverter Ingeteam Ingecon Sun 2.5 was determined in four different DC voltages. This inverter has lower efficiencies at lower DC input voltage and greater efficiencies in higher DC voltages. The percentage difference between the lowest and highest European and Californian efficiency was approximately 2.6% and 2.8%, respectively. Fig. 3 shows the values of European and Californian efficiency of inverter Ingeteam Ingecon Sun 2.5 for different DC input voltages.

The Fronius IG 30 inverter was tested in four different DC voltages. The lowest efficiencies were obtained in the lowest amount of DC voltage that the inverter has been tested, 160 V, while the highest values were obtained at 300 V_{DC}. The percentage difference between the highest and lowest European and Californian efficiency was 2.2% and 2.3% respectively. Table 6 shows the Fronius IG 30 inverter DC to AC efficiency in different DC voltages and for different loading levels. At levels of loading of 5% and at voltages greater than 300 V, the inverter provides efficiencies around 90% and maximum values of efficiency are achieved in loading levels of 50%.

The Sunways NT 4000 inverter was tested in seven different DC voltages. The highest efficiency values were obtained in the lowest DC voltage that the inverter has been tested, 370 V and the efficiency values decreased with increasing voltage. The percentage difference between the highest and lowest European and Californian efficiency were 1.6% and 1.9% respectively. Fig. 4 illustrates curves of efficiency of the Sunways NT 4000 inverter at different voltages.

The SMA Sunny Boy 3300TL inverter was tested at three different DC input voltages. The values of European and Californian efficiency increase proportionally with the DC voltage input. It is possible to find percentage deviations between the highest and lowest efficiency, about 4% and 3.7% in European and Californian efficiency, respectively. Table 7 shows the conversion efficiency of

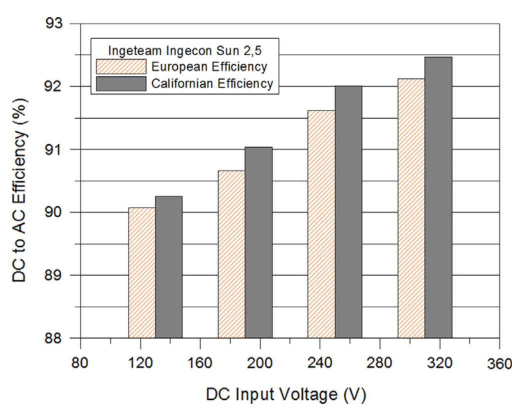


Fig. 3. European and Californian efficiency of Ingeteam Ingecon Sun 2,5 inverter in different voltages.

Table 6
Fronius IG 30 inverter efficiency in different DC input voltages and at different loading levels.

P_{AC}/P_{NOM} (%)	160 V	220 V	280 V	370 V
5	85.3	88.8	89.6	90.8
10	89.5	91.5	92.5	91.7
20	91.6	92.8	94.0	92.4
30	92.2	93.2	94.2	92.7
50	92.3	93.5	94.2	93.1
75	92.0	93.5	93.8	93.6
100	91.6	93.3	93.4	94.1

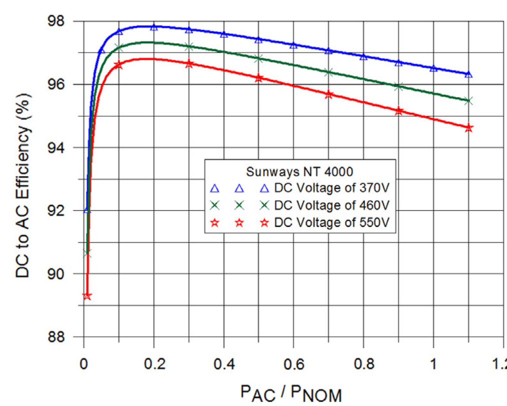


Fig. 4. Curves of conversion efficiency of the Sunways NT 4000 inverter in different voltages.

Table 7
DC to AC conversion efficiency of the SMA Sunny Boy 3300TL inverter in different DC voltages and for different loading levels.

P_{AC}/P_{NOM} (%)	250 V	400 V	550 V
5	86.3	88.0	89.6
10	91.8	93.2	94.3
20	94.2	95.6	96.5
30	94.5	96.0	97.1
50	93.7	95.8	97.2
75	92.6	94.9	96.8
100	90.4	93.8	96.3

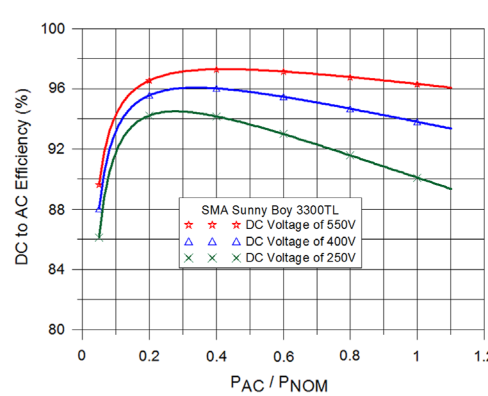


Fig. 5. DC to AC efficiency curves of the SMA Sunny Boy 3300TL inverter in different DC voltages.

the SMA Sunny Boy 3300TL inverter in different DC voltages and for different loading levels and Fig. 5 shows efficiency curves in different DC voltages.

4.3. Mathematical model of DC to AC conversion efficiency as function of the DC input voltage

The mathematical model of the Eq. (7) which describes the inverter DC to AC conversion efficiency curve is highly correlated with the experimentally measured data, however the model considers only the efficiency as a function of relative power. As the DC voltage also influences the behavior of the inverter efficiency curves, the mathematical model was modified to consider efficiency as a function of relative power and the DC input voltage, replacing the original coefficients K_0, K_1 and K_2 for linear combinations and new coefficients Eq. (13).

$$\eta_{inv} = \frac{(P_{AC}/P_N)}{(P_{AC}/P_N) + ((K_{0_{V_{DC0}}} \pm S_0 V_{DC}) + (K_{1_{V_{DC0}}} \pm S_1 V_{DC})(P_{CA}/P_N) + (K_{2_{V_{DC0}}} \pm S_2 V_{DC})(P_{CA}/P_N)^2)} \quad (13)$$

where P_N is the inverter nominal power; P_{AC} is the inverter output power; K_{0VDC}, K_{1VDC}, K_{2VDC} are voltage linear coefficients; S_0, S_1, and S_2 are voltage angular coefficients.

The coefficients K_0, K_1 and K_2 of the mathematical model, that considers the conversion efficiency as a function only of power present absolute values for each inverter and can be called power coefficients. However, the modified mathematical model presents the power coefficients as a function of DC input voltage. Each coefficient is described by two voltage coefficients, called voltage linear coefficient and voltage angular coefficient. Figs. 6–8 shows the behavior of the power coefficients K_0, K_1 and K_2 as a function of the DC voltage of the Ingeteam Ingecon Sun 2.5 inverter. Figs. 9–11 shows the behavior of the power coefficients K_0, K_1 and K_2 as a function of the DC voltage of the Xantrex GT 3.0 inverter. The voltage coefficients are determined from the fit between the theoretical curve, which in this case is linear, and the power coefficients determined in different DC input voltages.

From the determination of the voltage coefficients of the proposed mathematical model, conversion efficiency maps can be developed as a function of the DC voltage and relative power. The efficiency is determined from the mathematical model, at each point of DC voltage and relative power. These maps allow viewing the dynamic efficiency of the inverters as a function of DC voltage and relative power. Fig. 12 shows the map of Ingeteam Ingecon Sun 2.5 inverter efficiency depending on the DC voltage and relative power. The analysis of efficiency of the map shows that the highest efficiency values are obtained at voltages around 300 V and relative power between 30% and 70% while the lowest values of efficiency are obtained at voltages of about 120 V.

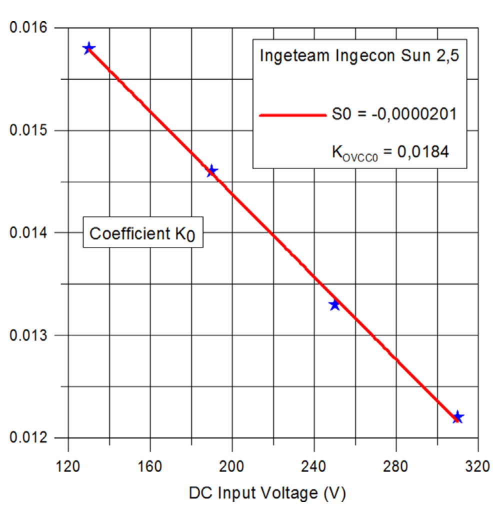


Fig. 6. Variation of K0 as function of DC voltage of the Ingeteam Ingecon Sun 2,5 inverter.

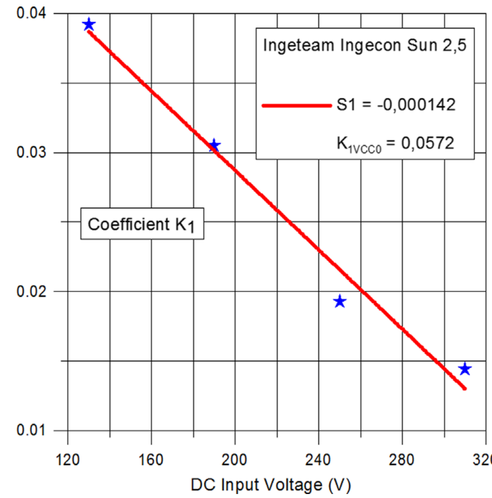


Fig. 7. Variation of K1 as function of DC voltage of the Ingeteam Ingecon Sun 2,5 inverter.

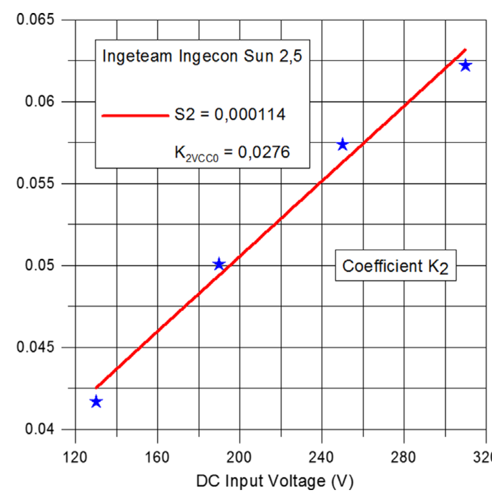


Fig. 8. Variation of K2 as function of DC voltage of the Ingeteam Ingecon Sun 2,5 inverter.

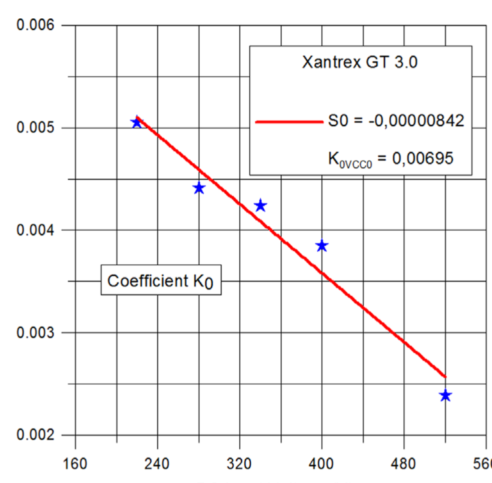


Fig. 9. Variation of K0 as function of DC voltage of the Xantrex GT 3.0 inverter.

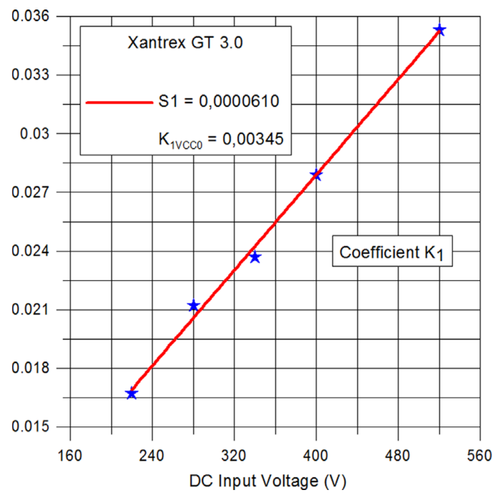


Fig. 10. Variation of K1 as function of DC voltage of the Xantrex GT 3.0 inverter.

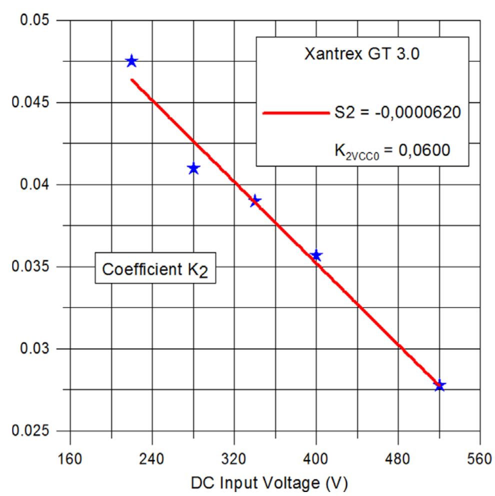


Fig. 11. Variation of K2 as function of DC voltage of the Xantrex GT 3.0 inverter.

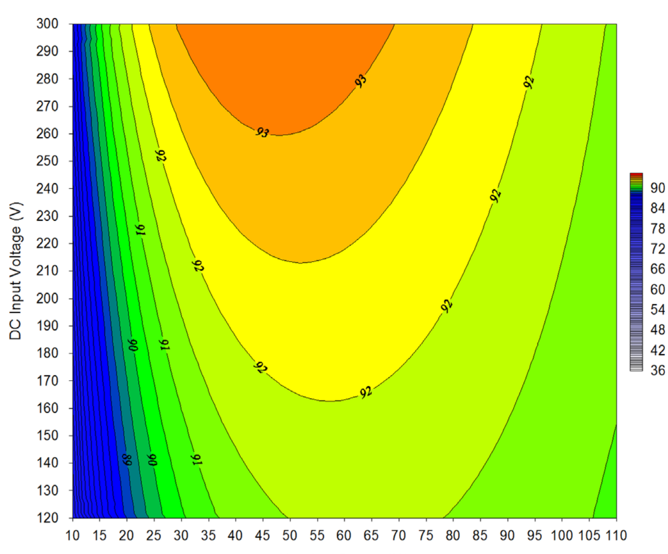


Fig. 12. Map of DC to AC efficiency of the Ingeteam Ingecon Sun 2,5 inverter.

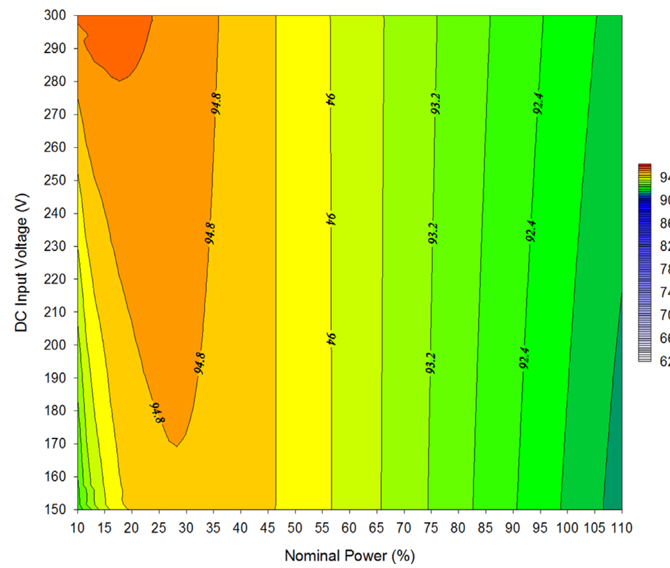


Fig. 13. Map of conversion efficiency of the SMA Sunny Boy 1100U inverter.

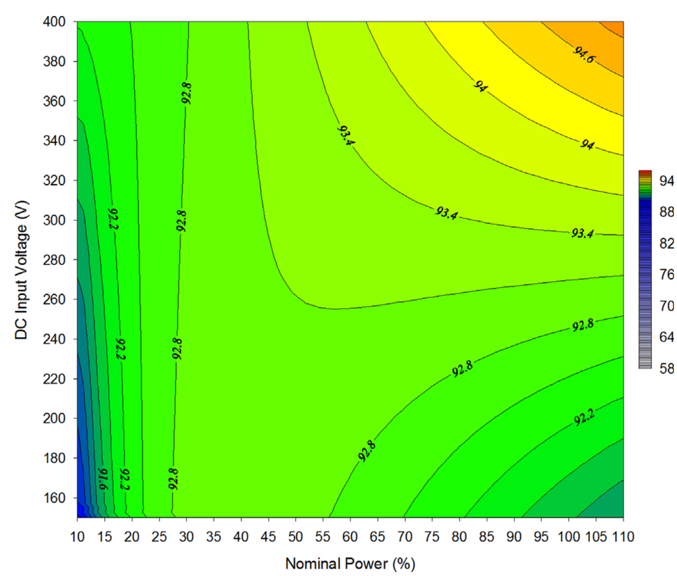


Fig. 14. Maps of conversion efficiency of the Fronius IG 30 inverter.

Fig. 13 shows the map of efficiency of SMA Sunny Boy 1100U inverter depending on the DC voltage and relative power. The analysis of efficiency map shows that the highest efficiency is obtained at voltages of about 300 V and relative power from 10% to 30% while the lowest efficiency are obtained from strains of the order of 150 V. The highest efficiency values, regardless of the DC input voltage, are obtained in relative power less than 50%.

The reverse process is also valid and can be used as a tool for a particular purpose. From the efficiency map of the inverter, it is possible to obtain the voltage coefficients of the mathematical model proposed to be inserted into a database software. Also from the efficiency curves at different DC voltages supplied by manufacturers of inverters it is possible to know the behavior of the variation of the coefficients as a function of power and DC voltage and then develop these maps. From the fit between the curves provided by the manufacturers and the curves provided by the mathematical model, power coefficients for each DC voltage can be determined, thus providing information about their behavior as a function of DC voltage and consequently the determination of the coefficients of the mathematical model proposed in this work. Figs. 14 and 15 show the maps of DC to AC conversion efficiency

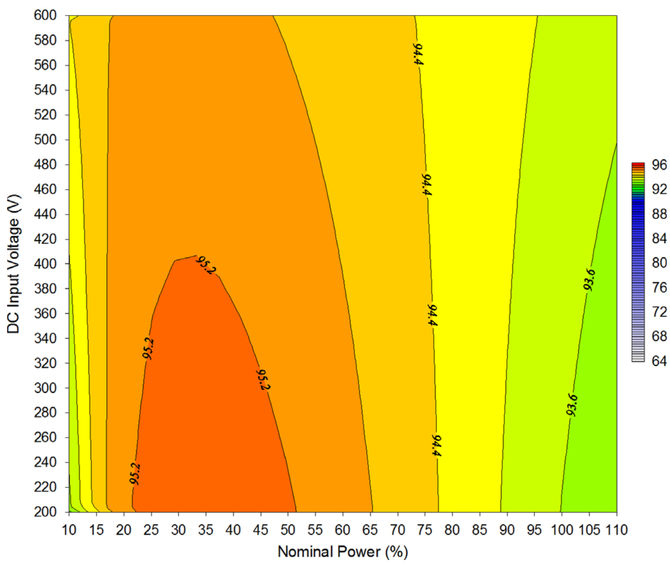


Fig. 15. Maps of conversion efficiency of the Xantrex GT 3.0 inverter.

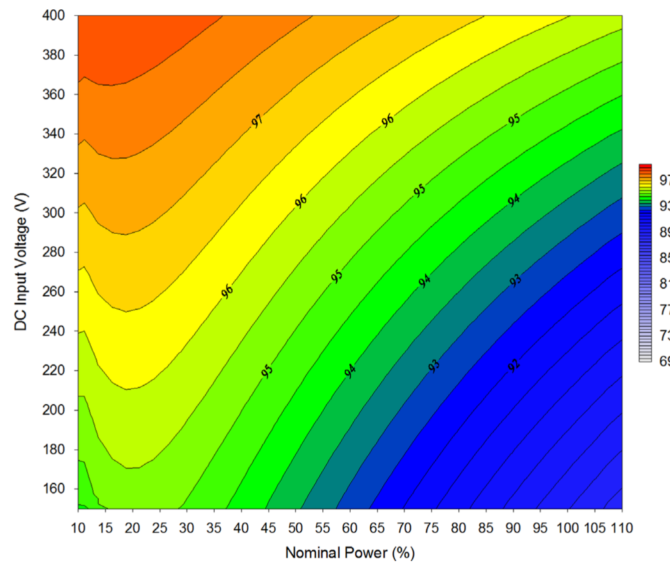


Fig. 17. Maps of conversion efficiency of the SMA Sunny Boy SWR 2000 inverter.

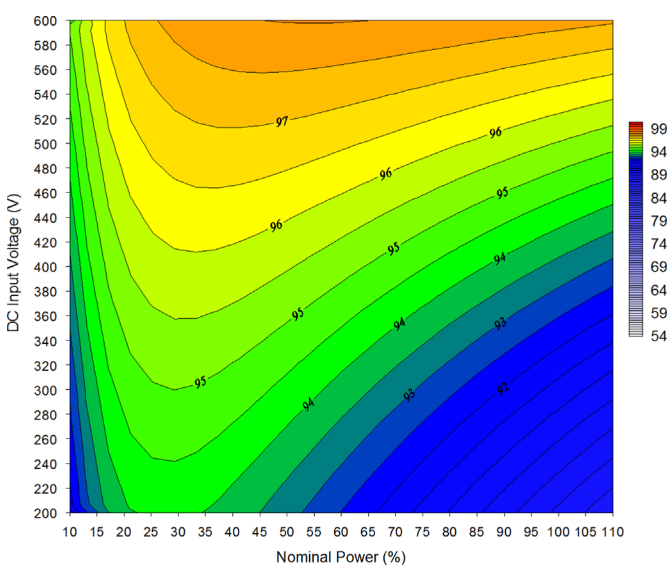


Fig. 16. Maps of conversion efficiency of the SMA Sunny Boy 3300TL inverter.

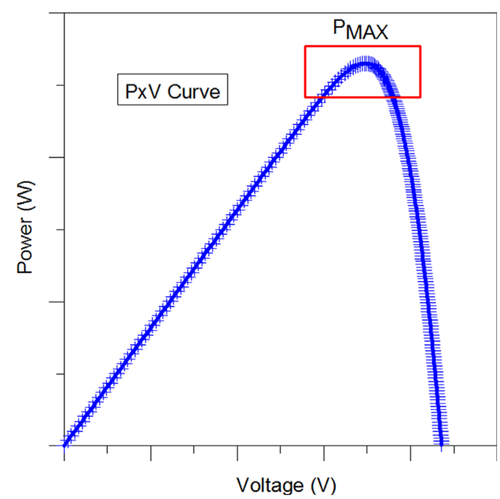


Fig. 18. Oscillating of DC voltage due to algorithm of inverter MPPT.

from Fronius IG 30 and Xantrex GT 3.0 inverters, respectively, and Figs. 16 and 17 show maps of conversion efficiency from SMA Sunny Boy 3300TL and Sunny Boy SMA SWR 2000 inverters, respectively.

4.4. *Tests of maximum power point tracker efficiency and proposed mathematical model*

The Standard IEC 50530, 2008, presents the definition and recommendation of the test conditions and measurement procedure for determining the static and dynamic MPPT efficiency of inverters. Measures should be taken throughout the range of permissible DC input voltage of the inverter and the relative power defined by European and Californian efficiency. The different tested inverters have different algorithms to track the maximum power point, though there are similarities between these algorithms. The PV array is biased by perturbing the operating voltage of the inverter. The interval between each perturbation varies with technology and the inverter manufacturer. The MPPT efficiency is a function of relative power. This parameter must be measured at different powers resulting in an efficiency curve of MPPT along the inverter range power. The static efficiency of the MPPT can be determined experimentally by adopting two assumptions:

- Assumption A: on a clear day (or during clear intervals along partially cloudy days) with no wind, the irradiance incident on the PV array and the temperature of the modules are constant within 1 min intervals.
- Assumption B: During the interval of 1 min, the MPPT inverter meets the PMP array at least 1 time (Fig. 18). The MPPT inverter is responsible for oscillating voltage during the interval of 1 min (Fig. 19).
- The input direct current and voltage of the inverter are continuously and simultaneously measured along 1 min. During each entire 1 minute period P_{MAX} is the value found for the highest power.

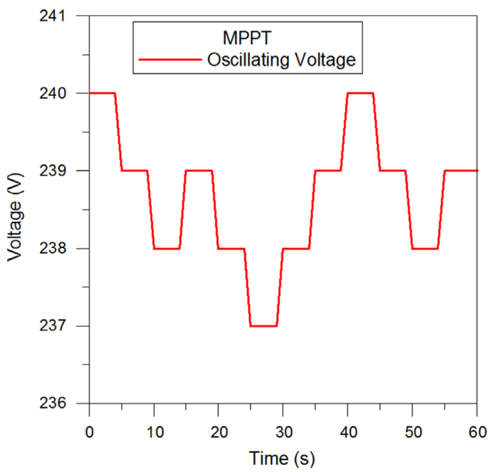


Fig. 19. Oscillating of DC voltage due to algorithm of inverter MPPT.

Table 8
Power coefficients of the mathematical model of MPPT static efficiency.

Technology	Model	Coefficients	
		M_0	M_1
Static efficiency of MPPT			
SMA	*SB* 700*U*	0.0075	0.0042
SMA	*SB* 2100	0.0022	0.0062
SMA	*SB* 3800*U*	0.0014	0.0055
SMA	*SB* 1100*E*	0.0085	0.0125
Fronius	*IG* 15	0.0039	0.0023
Fronius	*IG* 20	0.0027	0.0042
Fronius	*IG* 30	0.0028	0.0011
Mastervolt	*QS* 2000	0.0010	0.0115
Mastervolt	*QS* 3200	0.0035	0.0085

To determine the maximum power point tracker static efficiency of the inverter during 1 min Eq. (14) is used. This efficiency is approximately 99% of the tested inverters and can be considered constant in the operating range between 20% and 100% rated power of the inverter.

$$\eta_{\text{MPPT}} = \frac{\int_{r} VIdt}{\int_{r} P_{MAX}\, dt} = \frac{\sum_{i=1}^{n} V_i I_i \Delta t}{\sum_{i=1}^{n} n P_{\text{MAX}} \Delta t} \tag{14}$$

where V_i is the n values of measured voltage during the interval of 1 minute; Ii are the n values of measured during the current interval of 1 min; P_{MAX} is the maximum value of the pair (V_i, I_i) measured during the interval of 1 min.

A set of maximum power point tracker static efficiency data was obtained using the previously proposed method. Experimental data include measurements of inverters under different relative loads. The mathematical model presented in Eq. (15) was used for fitting theses data.

$$\eta_{inv} = \frac{(P_{DC}/P_{NOM})}{(P_{DC}/P_{NOM}) + (M_0 + M_1(P_{DC}/P_{NOM}))} \tag{15}$$

where M_0 and M_1 are power coefficients of the mathematical model that described the MPPT static efficiency curve.

Table 8 shows the coefficients of the mathematical model that represents the maximum power point static efficiency of the tested inverters and Table 9 shows the efficiency of the tested inverters for different values of power.

Table 9
Static Efficiency of MPPT of the tested inverters in different load levels.

	5%	10%	20%	30%	50%	75%	100%
SB 700*U*	86.6	92.6	95.9	97.1	98.1	98.5	98.8
SB 1100*E*	84.5	91.1	94.7	96.0	97.1	97.6	97.9
SB 2100	95.2	97.2	98.3	98.6	98.9	99.0	99.1
SB 3800*U*	96.7	98.0	98.7	98.9	99.1	99.2	99.3
IG 15	92.5	96.0	97.8	98.4	99.0	99.2	99.3
IG 20	94.5	96.9	98.2	98.6	99.0	99.2	99.3
IG 30	94.5	97.1	98.5	98.9	99.3	99.5	99.6
QS 2000	96.9	97.8	98.3	98.5	98.6	98.7	98.7
QS 3200	92.7	95.8	97.4	98.0	98.4	98.7	98.8

The MPPT static efficiency is nearly 100% in a wide power range and only in low power efficiency decreases to values between 85% and 96%, approximately, depending on the model and manufacturer of the inverter. The described method is valid for periods when the variability of the irradiance is less than 3%. In order to make the method valid even for periods in which variation of irradiance is greater than 3%, Eq. (16). must be applied. The MPPT dynamics efficiency consists of two terms, where the first term is MPPT static efficiency and the second term represents the condition of the irradiance variability. If the irradiance variation between two considered instants is null then the term variability is also null and dynamic efficiency will be equal to the static efficiency, but if there is variation in irradiance between the two moments considered the term variability is not null and dynamic efficiency will be lower the static efficiency. The term variability increases proportionally to the variation in the irradiance between the moments considered. On clear sky or overcast days the term variability is small but for partially cloudy days this term can be significant.

$$\eta_{\text{MPPT}} = \left(\frac{(P_{\text{DC}}/P_{\text{NOM}})}{(P_{\text{DC}}/P_{\text{NOM}}) + (M_0 + M_1(P_{\text{DC}}/P_{\text{NOM}}))} \right) - \left(M_2 \left(\frac{|P_2 - P_1|}{P_{\text{DC}}} \right) \right) \tag{16}$$

where M_2 is the power variation coefficient of the theoretical mathematical model which describes the curve of the MPPT dynamic efficiency; P_2 and P_1 are powers values at instants t_1 and t_2.

5. Conclusion

This work presented a study of inverters efficiency used in grid connected photovoltaic systems from theoretical and experimental tests. Experimental tests of inverters allowed the characterization of the DC to AC conversion efficiency, its dependence on the DC voltage and of the maximum power point tracker efficiency. The purpose of the tests was to measure and analyze various electrical characteristics of inverters in order to develop mathematical models that describe these characteristics. The inverters tests indicate that DC to AC conversion efficiency and MPPT efficiency are characteristics dependent on the power, but other variables such as DC input voltage may influence of these characteristics. The measured curves and the theoretical curves described by the proposed mathematical models, in general, presents R^2 determining coefficients greater than 0.9 indicating excellent correlation between measured points and theoretical curves. The characteristics were analyzed individually and the results aided understanding the process of interaction between the PV system and inverter and between the inverter and the grid.

References

[1] Dávilla L, Castro M, Amador J, Puerta D, Colmenar A. Sistema de Medida para el Modelado y Monitorizado de Generadores Fotovoltaicos Conectados a Red. In: 12th Congresso Ibérico y 7th Congresso Iberoamericano de Energia Solar, Vigo, Spain; 2004. p. 1049–54.
[2] Eltawil MA, Zhao Z. Grid connected photovoltaic power systems: technical and potential problems – a review. Renew Sustain Energy Rev 2010;14:112–29.
[3] Photon. Investigación y Tecnología: Inversores. La Revista de Fotovoltaica. Vol 3; 2010. p. 72–81.
[4] Patrao I, Figueres E, González-Spín F, Garcerá G. Transformerless topologies for grid-connected single-phase photovoltaic inverters. Renew Sustain Energy Rev 2011;15:3423–31.
[5] Salas V, Olías E. Overview of the state of technique for PV inverters used in low voltage grid-connected PV systems: inverters below 10 kW. Renew Sustain Energy Rev 2009;13:1541–50.
[6] González R, López J, Sanchis P, Marroyo L. Transformerless inverter for single-phase photovoltaic system. IEEE Trans Power Electron 2007;22(2):693–7.
[7] Kjaer SB, Pedersen JK, Fellow FB. A review of single-phase grid-connected inverters for photovoltaic modules. IEEE Trans Ind Appl 2005;41(5):1292–306.
[8] Salas V, Olías E. Overview of the State of Technique for PV Inverters used in Low Voltage Grid-Connected PV Systems: Inverters Above 10 kW. Renew Sustain Energy Rev 2011;15:1250–7.
[9] Khatib T, Mohamed A, Sopian K. A review of photovoltaic systems size optimization techniques. Renew Sustain Energy Rev 2013;22:454–65.
[10] Velasco D, Trujillo CL, Garcerá G, Figueres E. Review of anti-islanding techniques in distributed generators. RenewSustain Energy Rev 2010;14:1608–14.
[11] Ku Nurul Edhura Ku, Ahmad Jeyraj, Selvaraj Nasrudin Abd, Rahim. A. Review of the islanding detection methods in grid-connected PV inverters. Renew Sustain Energy Rev 2013;21:756–66.
[12] Khamis A, Shareef H, Bizkevelci E, Khatib T. A review of islanding detection techniques for renewable distributed generation systems. Renew Sustain Energy Rev 2013;28:483–93.
[13] Hassaine L, Olías E, Quintero J, Salas V. Overview of power inverter topologies and control structures for grid connected photovoltaic systems. Renew Sustain Energy Rev 2014;30:796–807.
[14] Zeng Z, Yang H, Zhao R, Cheng C. Topologies and control strategies of multi-functional grid connected inverters for power quality enhancement: a comprehensive review. Renew Sustain Energy Rev 2013;24:223–70.
[15] International Electrotechnical Commission (IEC 61683). Photovoltaic systems – power conditioners – procedure for measuring efficiency; 2008.
[16] King DL, Gonzalez S, Galbraith GM, Boyson WE. Performance model for grid-connected photovoltaic inverter. Sandia National Laboratories, Sandia Report; .
[17] Keating L, Mayer D, McCarthy S, Wrixon GT. Concerted action on computer modeling and simulation. In: European Photovoltaic Solar Energy Conference, Lisbon, Portugal; 1991.
[18] Chivelet NM, Chenlo-Romero F, Alonso-Garcia MC. Modelado y Fiabilidad de los Inversores para Instalaciones Fotovoltaicas Autónomas a partir de Medidas con Cargas Resistivas y Reactivas. In: 7th Congresso Ibérico de Energía Solar, Spain; 1994. p. 463–8.
[19] Jantsch M, Schimidt H, Schmid J. Results of the concerted action on power conditioning and control. In: Proceedings of the 11th European Photovoltaic Solar Energy Conference, Montreux, Suiça; 1992. p. 1589–93.
[20] International Electrotechnical Commission (IEC 50530). Overall efficiency of photovoltaic inverters; 2008.
[21] Alonso-Abella M, Chenlo F. Choosing the right inverter for grid-connected pv systems. Renew Energy World 2004;7:132–47.
[22] García M, Maruri JM, Marroyo L, Lorenzo E, Pérez M. Partial shadowing, MPPT performance and inverter configurations: observations at tracking PV plants. Prog Photovolt: Res Appl 2008;16:529–36.
[23] Sanchis P, López J, Ursúa A, Gubía E, Marroyo L. On the Testing, characterization, and evaluation of PV inverters and dynamic MPPT performance under real varying operating conditions. Prog Photovolt: Res Appl 2007;15:541–56.
[24] De Cesare G, Caputo D, Nascetti A. Maximum power point tracker for portable photovoltaic systems with resistive-like load. Sol Energy 2006;80:982–8.
[25] Duru HT. A maximum power tracking algorithm based on $I_{MPP}=f(P_{MAX})$ function for matching passive and ative loads to a photovoltaic generator. Sol Energy 2006;80:812–22.
[26] Salas V, Olías E, Lázaro A, Barrado A. New algorithm using only one variable measurement applied to a maximum power point tracker. Sol Energy Mater Sol Cells 2005;87:675–84.
[27] Huang BJ, Sun FS, Ho RW. Near Maximum Power Point Operation (nMPPO) Design of photovoltaic power generation system. Sol Energy 2006;80:1003–20.
[28] Noguchi T, Matsumoto H. Maximum power point tracking method of photovoltaic power system using a single transducer. Electr Eng Jpn 2007;160(n. 1):54–9.
[29] Tokushima D, Uchida M, Kanbei S, Ishikawa H, Naitoh H. A new MPPT control for photovoltaic panels by instantaneous maximum power point tracking. Electr Eng Jpn 2006;157(3):73–80.
[30] Kawamura T, Harada K, Ishihara Y, Todaka T, Oshiro T, Nakamura H, Imataki M. Analysis of MPPT characteristics in photovoltaic power system. Sol Energy Mater Sol Cells 1997;47:155–65.
[31] Bhatnagar P, Nema RK. Maximum power point tracking control techniques: state of the art in photovoltaic applications. Renew Sustain Energy Rev 2013;23:224–41.
[32] Caamaño-Martín E. Edificios Fotovoltaicos Conectados a La Red Eléctrica: Caracterización y Análisis [Doctoral thesis]. Spain: Escuela Técnica Superior de Ingenieros de Telecomunicación, Universidad Politécnica de Madrid; 1998.
[33] Gergaud O, Multon B, Ahmed HB. Analysis and experimental validation of various photovoltaic system models. In: Proceedings of the 7th International Electrimacs Congress, Montreal; 2002.
[34] Fronius IG. Operating instructions: grid-connected inverters for photovoltaic systems; 2005.
[35] Mastervolt. Users and installation manual sunmaster QS 2000: grid connected solar inverter; 2006.
[36] Mastervolt. Users and Installation Manual Sunmaster QS 3200: grid connected solar inverter; 2005.
[37] SMA Solar Technology AG. Installation Guide Sunny Boy 2000/2500: string inverter for photovoltaic plants; 2007.
[38] SMA Solar Technology AG. Installation Guide Sunny Boy 3800U; 2005.
[39] SMA Solar Technology AG. Installation Guide Sunny Boy 700U: photovoltaic, grid-tied string inverter; 2003.
[40] Kreutzmann A, Welter P. Market survey on inverters for grid-tied PV systems. PHOTON Int – Photovolt Mag 2005;4:88–95.
[41] Ingeteam.. Ingecon Sun Inversores Conectados a Red – Uma Família Completa de Inversores para la Conexión a Red de Plantas Fotovoltaicas; 2008.
[42] Sunways Photovoltaic Technology. Solar invertir; 2007.
[43] Xantrex Technology. Xantrex grid tie solar inverter – Owner's 2007; 2007.
[44] Girbau Z, Chenlo F, Caamaño-Martin E. Comparación de dos sistemas FVS distintos conectados a rede en la misma localidad. In: 12th Congresso Ibérico y 7th Congresso Iberoamericano de Energia Solar, Vigo, Spain; 2004, p. 1031–6.